Journal of Optoelectronics and Advanced Materials Vol. 6, No. 2, June 2004, p. 359 - 384

REVIEW PAPER

PHOTODESORPTION OF MOLECULAR ADSORBATES FROM METALLIC SURFACES

D. Bejan*

Bucharest University, Faculty of Physics, Department of Optics, P.O. Box MG-11, 077125-Bucharest, Romania

Photoinduced processes at surfaces are intimately connected with the dynamics of electrons and energy flow between substrate and adsorbate. Rapid progress in the experimental field, achieved with the advent of ultra-short laser pulses of high intensity and a wide range of excitation energy, stimulated a surge of various theoretical models. Desorption from metal surfaces exhibits some general properties like nonlinear yield dependence as function of the laser fluence, short desorption times, specific final state distribution. These characteristics are related to excitation or relaxation processes driven by the substrate carriers. In this review we present a panorama of classical and quantum models developed to describe photodesorption process at surfaces. As a specific example, we present the widely studied desorption of CO molecule from metallic surfaces.

(Received February 24, 2004; accepted April 14, 2004)

Keywords: Desorption, Laser, Metal surfaces, Wave packet, Density matrix, Nonlinear yield

1. Introduction

The nature of interaction and the rate of energy flow between an adsorbate and a solid surface constitutes key issues in surface dynamics. Despite considerable experimental and theoretical efforts, a complete understanding of the interaction between the localized excitation of the adsorbate and delocalized electronic and lattice excitation in the substrate remains elusive. For metal surfaces, strong coupling is generally present and typical relaxation rates lie in the picosecond to femtosecond domain. While these processes cannot be examined in real time using conventional surface science probes, recent laser-based techniques provide the possibility to study the adsorbate-substrate interaction in time-domain. Furthermore, the combination of two important techniques like time-resolved laser spectroscopy and scanning tunneling microscopy (STM) provides a promising approach for simultaneous spatial and temporal resolution of optically initiated processes at interfaces [1].

The excitation of the adsorbate-substrate complex can be categorized into two classes. Under the laser action, a direct excitation of the adsorbate by the photon may be produced. This is similar to a gas phase process and often occurs on insulator surfaces, which are transparent to the incident light. On the contrary, on metal and some semiconductor surfaces, the photochemistry is triggered by photon absorption by the substrate from the near IR to near UV energy range (see the next section). This absorption results in excitation of electrons above the Fermi level, becoming hot electrons. These non-thermal carriers can diffuse from the creation point, in the volume or at the surface, to attach to the adsorbate. If there is an energetic barrier between the surface and the adsorbate then this process can involve tunneling through it. As in the gas phase, the adsorbate and the electron can eventually form a resonant negative ion. Excitation in the same energy range can be achieved by electron impact with electrons coming from an electron gun [26,87,88] or from a tip of a scanning tunneling microscope [89] giving rise to the electron stimulated desorption (ESD). In the following, these different excitations (electron or photon stimulated) are discussed together.

* Corresponding author: dbejan@easynet.ro

Because of the fast relaxations processes, the lifetime of the transient species on metal surfaces is usually very short (1-100 fs) preventing the efficient energy exchange between the electronic and nuclear motion and giving rise to low desorption probability. For example, desorption was not obtained for Ni surfaces while for Cu or Ru desorption was observed only using subpicosecond laser pulses [2,3].

Secondary chemical and physical processes may ensue despite the competing relaxation. The adsorbate may perform a hindered rotation, be vibrationally excited, diffuse across the surface, desorb and dissociate or undergo chemical reactions with the metal surface. Final state distribution of the various translational and internal degrees of freedom, angular distribution and population of the spin-orbit states can be analyzed experimentally to unravel the underlying dynamics.

Experiments and mechanisms of photo-stimulated surface processes have been extensively reviewed in the past. For more detailed accounts, the reader is referred to the original literature, beginning with the pioneering paper by Chuang [4], a comprehensive review of photo-induced reactions at metal surfaces by Zhou, Zhu and White [5] and an extensive report on state-resolved experiments and studies by Zimmerman and Ho [6]. The book edited by Dai and Ho [7] provided a panoramic view of surface photochemistry. The recent review of Guo, Saalfrank and Seideman [8] discussed the various theoretical models used to investigate two prototypical problems in which the substrate dictates different excitation and relaxation mechanisms. On one side, these authors investigated desorption from insulator surfaces where the interaction with the substrate is weak and the substrate induced relaxation is slow. On the other side, they treated the dynamics of the adsorbate at metal and semiconductor surfaces where there is a strong electronic coupling between adsorbate and substrate, responsible for the rapid relaxation of both electronic and vibrational degrees of freedom. Very recently, Seideman [117] reviewed the theoretical and experimental work on the dynamics induced in molecular scale devices like molecular heterojunctions, molecular wires, single molecules confined between a substrate and a tip, conducting molecules isolated in insulating monolayers. The formalism is applied to single molecule-surface reaction induced by STM and current-triggered dynamics in molecular nano-devices. The underlying conductance in molecular devices is related to desorption because it concerns nuclear dynamics induced by transient electronic excitations, similar to processes appearing in desorption.

The present review is designed to provide a thorough discussion of the theoretical models from the point of view of an important hallmark of all desorption experiments that is the nonlinearity of desorption yield with the laser fluence. The review is limited to well characterized metal surfaces and the theories are tested on CO - the prototype adsorbate molecule - desorption, processes well investigated from the experimental and theoretical points of view. In Section 2, we give an overview of the desorption experiments and discuss their particularities that conducted finally to consider desorption from metal surfaces as mediated by the substrate electrons. Theoretical methods, including time-dependent and time-independent quantum methods, classical and semiclassical trajectory methods, are detailed in Section 3. Specific models and their results are presented for CO on different metal surfaces in Section 4. Concluding remarks are given in Section 5.

2. An overview of the experiments and their interpretation

Desorption induced by picosecond and femtosecond laser pulses has been studied for several systems: NO/Pd(111) [9-11], NO/Pt(111) [12-14], CO/Cu(111) [2] and CO/Cu(100) [15], CO/Pt(001) [16,17], CO/Pt(111) [18], CO/Ru(001) [3], O_2/Pd(111) [19-21], O_2/Pt(111) [22,23], NH_3/Cu(111) [24].

The performed experiments are almost of the pump-probe type or two-pulses correlation type. In most of the experimental pump-probe approaches, the extraction of the dynamical information starts with a short-pulsed laser (pump laser). The pump laser duration must be shorter or of the same order of magnitude as the duration of the studied process. These pump lasers are usually dye systems or solid-state systems such as titanium-doped sapphire (Ti:sapphire) [25]. Synchronously pumped dye-lasers are widely tunable but require dyes changes to cover a wide wavelength region. In these systems, the 1.06 μm light from a CW-mode-locked Nd:YAG laser is frequency doubled to 532 nm and pumps a dye laser. Pulses as short as 150 fs are achievable.

Ti:sapphire systems are relatively new and provide intense pulses with broad tunability from 700 nm to over 1000 nm. Very short pulses of 4 fs have been reported. The desorbing molecules are probed with a tunable dye laser (probe laser) using Laser Induced Fluorescence (LIF) or Resonant Enhanced Multi Photon Ionization (REMPI) techniques. The pump laser is usually oriented normal to the surface whereas the probe one is parallel to it and located at a typical distance of few millimeters. Kinetic energy distribution for the molecules being in a specific rotationally and vibrationally state were determined from time of flight (TOF) spectra measured by varying the delay time between the two laser pulses while the probe laser frequency was fixed at the desired molecular state of the desorbed molecule. Internal state distribution for particles within a given velocity interval were obtained from the excitation spectra recorded by varying the frequency of the probe laser for a fixed time delay.

In the two-pulses correlation scheme, the total desorption yield is measured as function of temporal separation between a pair of excitation pulses. To minimize interference effects, the two beams have orthogonal polarization. In this manner one obtains femtosecond time resolution despite the large time delay required for the desorbed molecules to be detected [15,23].

The second harmonic generation (SHG) method, also used to determine the desorption yield [2], measures in fact the polarizability change of the surface atoms and therefore probes the molecules that remained on the surface, being sensitive to the coverage. The signal increases with the diminishing coverage and stabilizes at a constant value afterward. The time needed to reach the constant value was identified as the duration of the desorption event. It is not a direct measure of the photodesorption time because, to be counted as photodesorbed, the molecules should leave the interaction region.

Some general properties have been observed in these studies. The most outstanding characteristic is the nonlinear dependence of the desorption yield with the laser fluency. For comparable fluence, significant enhancement of the desorption yield in picosecond laser pulses experiments relative to nanosecond ones and a picosecond response time for desorption were observed. Also, final state energy distribution exhibits nonthermal rotational population that can be converted to a very high mean rotational temperature and also a very high vibrational temperature [15]. However the translation is excited only slightly and corresponds to a relatively modest translational temperature. These observations are inconsistent with a conventional thermal or photochemical mechanism of desorption, and have been attributed to a desorption process driven by the high degree electronic excitation of the substrate.

The mechanism of photodesorption, almost generally adopted, is close to the ideas of Gadzuk [14]. The laser excites first the electrons of the metal creating a bath of hot, nonequilibrium, electrons that will scatter into an unoccupied valence electron resonance of the adsorbate forming a temporary negative ion. After the neutralization of the negative ion, the system returns to the ground state of the adsorbate and an excited state of the substrate located in the conduction band of the metal. During the excitation/relaxation process, energy is gained by the adsorbate in both internal and desorption coordinate. Hence the adsorbate can desorb and/or dissociate.

What are the arguments sustaining the key role of the substrate electronic excitation in the desorption mechanism? The first argument is that the desorption yield scales quantitatively with the amount of radiation absorbed by the metal and not with the magnitude of the electric field normal or parallel to the surface [10,14]. Thermal desorption (TD) spectra of molecular oxygen absorbed on Pd(111) excited by nanosecond lasers [21], show strong similarities for all the laser energies used in the experiment (3.9, 5.0, 6.4 eV). This fact indicates that the first step of excitation cannot take place in the adsorbate. At low coverage, where the interaction between the adsorbed molecules is negligible, the molecular levels are discrete and a strong dependence on the laser energy is expected if the direct intramolecular transitions play a role in the desorption mechanism. Because of the lack of excited states, the energy (around 2 eV) commonly used in the experiments is too low to justify a

direct light adsorption in the adsorbate. Only an indirect adsorbate excitation, by the primary excited electrons of the substrate, can explain these experimental findings.

The very short time response, less than 1 ps found for NO/Pd(111) [10] and O_2/Pt(111) [23] or even less than 325 fs found for CO/Cu(111) [2], rule out all mechanisms in which the turn-on or turn-of times would be too slow. This eliminates all the thermal or thermal assisted (caused by the phonons) mechanisms since desorption is completed even before the lattice heats up (about 1-2 ps). This eliminates also, all mechanisms of desorption that are driven by local vibrational modes (surface phonons or the adsorbate-metal vibration) thermally equilibrated with the hot electrons through their coupling, because the desorption rate would be too slow. Only processes driven by the electrons can produce such a fast desorption dynamics. However, some experiments indicate that vibrational relaxation on metal surfaces can be rather fast because of strong coupling with the substrate electron-hole pairs [118].

All the photodesorption experiments performed in the subpicosecond range [2,3,9,10,11,15,19,21] but also some of the experiments performed in the nanosecond range [16,17] put in evidence a power-law yield dependence on the laser fluence, $Y \sim F^n$, with n between 2 and 8. This superlinear yield dependence on the laser fluence cannot be explained by coverage-dependent desorption kinetic effects. The yield dependence could be explained in this way if the desorption got easier with decreasing coverage but, for example, for CO/Cu(111) [2] it has been found the opposite: CO gets slightly harder to desorb as the coverage decreases. Also, a direct intramolecular excitation or a direct excitation metal to an adsorbate unoccupied state are excluded because they would give a linear dependence of the yield on the adsorbed laser fluence. In order to explain the superlinear yield dependence a mechanism of multiple excitations of the adsorbate by the electrons of the substrate (desorption induced by multiple electronic transition, DIMET) was proposed and will be detailed further below in section 3.1.3.

3. An overview of the theoretical models

3.1 Time-dependent wave packet methods

3.1.1 MGR and Antoniewicz models

The first proposed quantitative approach for nonthermal desorption is the well known Menzel-Gomer-Readhead (MGR) model presented independently in 1964 by Menzel and Gomer [26] for electron stimulated desorption and by Readhead [27] for photon stimulated desorption of adsorbates from metallic surfaces. It is essentially a two-state, one dimension (1D) model, where the electronic transitions are instantaneous. It can be explained on the basis of Fig. 1, where several potential curves are shown, function of the desorption coordinate z: the electronic ground state of the metal-adsorbate system (M+A) (M: metal, A: adsorbate), a neutral antibonding state $(M+A)^a$, an ionic state (M^-+A^+) -with an equilibrium bond length larger than that of the ground state- and two metastable states where the metal is excited and the adsorbate is in its ground state $(M+A)^*$. For metallic substrates, the continuous of electron-hole excitations allows the continuous displacements of the last curve. Electronic excitation and deexcitation processes are considered as vertical Franck-Condon (FC) transitions. The desorption process can be started by a FC transition from (M+A) to the antibonding neutral state, $(M+A)^a$. If no relaxation into the ground state takes place, the particle moves on the repulsive potential curve and desorbs. On the contrary, if electronic de-excitation to the substrate occurs, the particle returns to the ground state but it has gained some kinetic energy while moving on the repulsive potential. If this energy is higher than the desorption threshold, the adsorbate can desorb. Otherwise it is trapped on an excited vibrational state of the ground state. A second possibility is due to the electrostatic interactions between the two diabatic states $(M+A)^a$ and $(M+A)^*$ near the crossing point. Generally, curves crossing may give rise to processes like

tunneling, deexcitation and/or reneutralization. In the present case, the particle can be temporary trapped in the bonding excited state $(M+A)^*$. If the particle has accumulated enough kinetic energy, it desorbs leaving the surface in its ground M or in an excited M^* state. Another case is the excitation to the ionic state (M^-+A^+) where the same processes described above can take place.

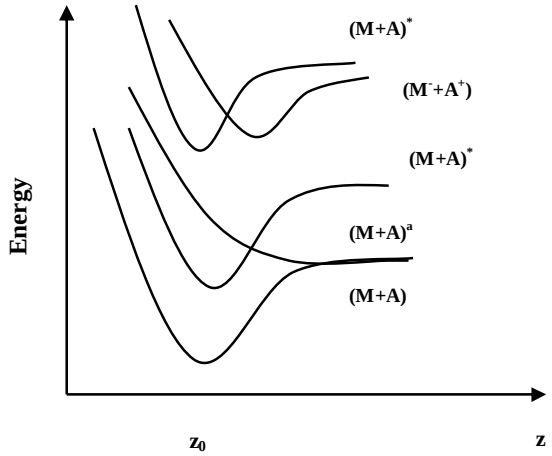

Fig. 1. Diabatic representation of possible potential energy curves within the MGR model. (M+A) corresponds to the ground state configuration, $(M+A)^a$ to the antibonding state, (M+A)* to the excited state (metastable) and (M^-+A^+) to the ionic state. The possible curve crossings are also illustrated.

MGR is in essence a semiclassical model: the excitation-deexcitation processes are modeled quantum mechanically and the nuclear motions are described classically. For example, after excitation to the higher energy curve (corresponding to the antibonding, ionic or metastable states) the particle moves toward the substrate with a classical velocity: $v(z)=\{(V(z_o)-V(z))/M\}^{1/2}$ where M is the particle mass, V(z) is the excited state potential and z_0 is the equilibrium point. The total desorption probability predicts a strong mass dependence and consequently a strong isotope effect:

$$P_e = \exp\left[-(M/2)^{1/2}\int_{z_0}^{z_c}\frac{R(z)}{(V(z_0)-V(z))^{1/2}}dz\right], \quad (1)$$

where, depending on the effective processes involved in Fig. 1, R(z) is the hopping and/or tunneling probability. The integral is performed from the equilibrium point z_0 to the critical distance z_c. If the deexcitation occurs before the system reached this distance, the particle will desorb. Otherwise it is recaptured. One observes that desorption dynamics is governed by the repulsive parts of the excited states potentials.

Antoniewicz [28] proposed a slightly modified 1D model for particles physisorbed on metallic surfaces. In this case one creates $(M^+ + A^-)$ or (M^-+A^+) ionic states with an equilibrium bond length shorter than the ground state, due to the attractive Coulomb interaction between the charge of the ionic adsorbate and its image produced by the metallic surface. The FC transition places the particle on the attractive part of the ionic potential curve and the acceleration is now toward the surface, accumulating kinetic energy E_{kin}. The relaxation time to the ground state is short compared to the metal-adsorbate vibrational period and the adsorbate jumps to the ground state before reaching the repulsive branch of the potential. If this relaxation time is sufficiently long to allow accumulation of enough kinetic energy (beyond the desorption threshold of the ground state) desorption occurs and the particle leaves the surface eventually with some translational energy E_{trans}. This model is

different from the MGR model only by the position of the potential curves and therefore the probability is also given by the eq. (1).

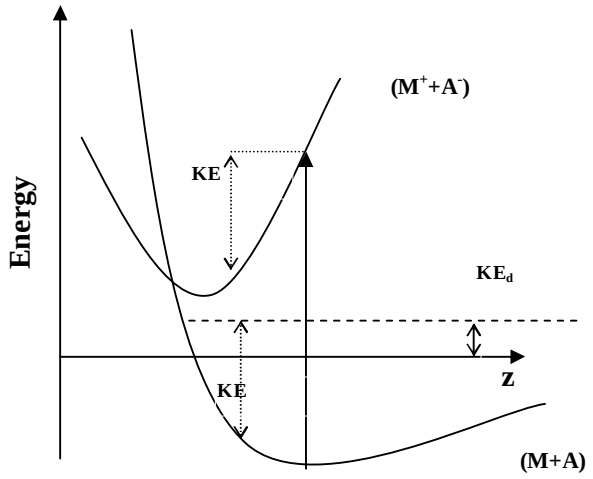

Fig. 2. Desorption mechanism in the Antoniewicz model. KE is the kinetic energy acquired during the motion in the ionic state (M^++A^-) and KE_d is the translational energy of the desorbing molecule.

The above models have an important drawback: they cannot reconcile the values of the desorption yield and of the kinetic energy. If the lifetime of the excited state is chosen such that the calculated kinetic energy of the desorbing particle agrees with the observed one, then the calculated yield is too small. However, when increasing the lifetime the gain of kinetic energy becomes too large. This shortcoming still persists in a fully quantum version of desorption that follow closely the classical one [29]. Moreover, in the MGR and Antoniewicz models there is no explicit introduction of the band structure of the solid and the electronic relaxation is treated as an instantaneous transition after a fixed time delay to another PEC. In reality, the quenching is a continuous process, determined on a microscopic level by the specific electron dynamics. Gortel [29] introduced the continuum of potential energy curves (PECs) parallel to the ground state that corresponds to the continuum of energy levels of the metallic bands, thus leading to a more realistic representation of the metal structure. Consequently, the density of states and the bandwidth were included in the calculus of the neutralization rate [30]. Another quantum mechanical extension of the Antoniewicz model was proposed by Hubner and Brenig [31]. They used an optical potential (related to the neutralization rate) to couple the two states, thus modeling the dissipation of the energy to the substrate.

An interesting quantum mechanical extension of desorption scenario, called wave-packet-squeezing (WPS) [32, 33], was proposed by Gortel. This author considered the potentials of the ground and excited state having the same equilibrium positions but the latter PEC has a different shape: it is deeper and narrower than the former one. The kinetic energy increases in the excited state by a dynamical squeezing of the wave packet representing the adsorbed particle. The increased localization of the wave packet leads to larger momentum uncertainty of the particle and, consequently, to the increase of the kinetic energy: $2m < E_{kin}(t) >=< p(t) >^2 +(\Delta p(t))^2$. The $< p(t) >^2$ contribution evolves according to the classical mechanics and is present in an Antoniewicz-type model, while the term containing the momentum uncertainty $\Delta p(t)$ represents a purely quantum contribution to the kinetic energy. For nearly coincident equilibrium positions of both potentials only $\Delta p(t)$ increases, leading to desorption. This situation applies if the relaxation

time is longer than the particle-surface vibrational time and the wave function becomes stationary in the excited state 'forgetting' its origin.

3.1.2 Gadzuk model

In the models described above, there were considered neutral excited or charge transfer from adsorbate to metal ($M^- + A^+$) states. But the excitation energy of these last states is large (> 10 eV for diatomic adsorbate molecules) and is not reached by the present standard subpicosecond lasers. Gadzuk [14] have suggested an inverse charge transfer ($M^+ + A^-$) that corresponds to a much lower energy (few eV). In fact, as mentioned in section 2, in this model the laser excites first the electrons of the metal creating a bath of hot, non-equilibrium, electrons that will scatter into an unoccupied valence electron resonance of the adsorbate forming a temporary negative ion. As displayed in Fig. 3(a) the hot electrons populate the empty molecular orbital $2\pi^*$ of the adsorbed NO, lying above the Fermi level of the NO/Pt system. During its characteristic decay time τ_r the wave packet moves on the negative ion potential $V_-(z)$ (Fig. 3(b)) until the relaxation to the ground state V_0 takes place. The relaxation time determines the dispersion of the wave packet and the kinetic energy distribution. Also, it determines the excitation of the adsorbate-surface vibration due to the displacement of the ionic state potential with respect to the ground state one.

As Hubner and Brenig [31] did before, Gadzuk uses for the ground state potential V_0, a Morse potential:

$$V_0(z) = D[1 - \exp(\beta_0 z)]^2 \tag{2}$$

and for the excited state V_-, an additional image-potential is turned on because the state is charged:

$$V_-(z) = \varepsilon^* + V_0(z) - e^2 / 4(z + z_{eq}) . \tag{3}$$

Here $\varepsilon^* = \phi - A$ is the substrate work function minus the electron affinity and z_{eq} is the distance between the image plane and the equilibrium position of the adsorbate (NO^- in the present case). This highly simplified model for the negative ion potential curve is based on the *ab-initio* calculations of Avouris et al. [34] who studied stimulated desorption path of fluorine on Al. This simplified form for the ground and ionic potentials is generally used in all the other desorption models.

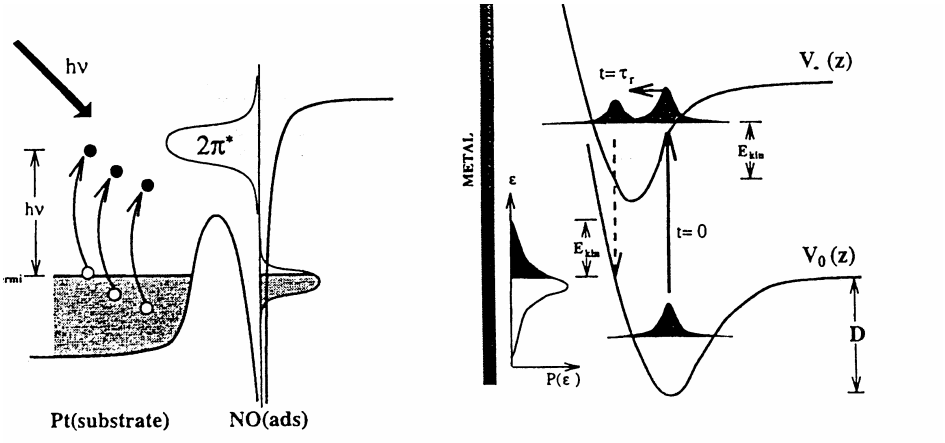

Fig. 3. Gadzuk model of photodesorption. Two representations of the same process for NO/Pt(111). (a) Electrons of the solid are excited by the photon above the Fermi level into the $2\pi^*$ level, forming the negative molecular ion NO^-. (b) The photons transfer the ground state wave packet to the negative ion state with its associated PEC $V_-(z)$. The wave packet propagates on $V_-(z)$ during a characteristic time τ_r, then it decays to the ground state and desorbs. From Gadzuk et al. [14].

The "jumping wave packet" method [14] proposed by Gadzuk consist of: (i) the initial preparation of $|\psi(t=0)\rangle = |\psi_0\rangle$, the harmonic oscillator ground state of V_0, as a stationary state of V_- at t = 0; (ii) the prepared wave packet $|\psi(t)\rangle$ is transferred to the excited state and evolves on the ionic potential V_-. After a time t, the wave function is given by the evolution operator $|\psi(t)\rangle = \exp(-iH_- t/\hbar)|\psi(t=0)\rangle$, where $H_-=T+V_-$ and T is the kinetic energy operator; (iii) after a time τ_r, corresponding to the lifetime of the excited state the wave packet return on V_0 as a non-stationary state of the ground potential; (iv) subsequent evolution on this state in accordance with the equation $|\psi(t';\tau_r)\rangle = \exp(-iH_0 t'/\hbar)|\psi(t'=0;\tau_r)\rangle$. Assuming an exponential decay of the resonance, Gadzuk suggested to run different wave packets corresponding to different residence times τ_r on the excited state surface, and subsequently to average incoherently over individual operator expectation values weighted by a function *w* falling in time (e.g. $\exp(-t/\tau_r)$, [35,58,116]). In practice the residence time τ_r can be chosen on a discrete grid (equidistant or random) and the averaged quantities are obtained as:

$$\langle A(t)\rangle = \sum_{n=1}^{N} w_n \langle \psi(t;\tau_{rn})|A|\psi(t;\tau_{rn})\rangle, \tag{4}$$

where the discrete weighting factor w_n associated to each τ_{rn} is a predetermined analytic function falling in time.

In the short time limit (τ_r relevant but short), Gadzuk showed [36] that the excited state potential V_- can be linearized and consequently, $|\psi_0\rangle$ returns to the ground state V_0 as a Gaussian wave packet:

$$|\psi(t'=0;\tau_r\rangle = \exp\{i/\hbar[\alpha_{\tau_r}(z-z_{\tau_r})^2 + p_{\tau_r}(z-z_{\tau_r}) + \gamma_{\tau_r}]\} \tag{5}$$

where the width α_{τ_r}, the packet center z_{τ_r}, momentum p_{τ_r} and phase γ_{τ_r} are all function of the residence time τ_r and evolves according to four specific equations. The evolution of the wave packet center of gravity and momentum obey the classical Hamilton's equations [37]:

$$\frac{dz}{dt} = \frac{\partial H}{\partial p}; \frac{dp}{dt} = -\frac{\partial H}{\partial z}. \tag{6}$$

In this hypothesis, simplified expressions can be found for the desorption probability $P_{des}(\tau_r)$. Such a Gaussian wave packet propagation scheme has been also used by Shuck and Brenig [38] and Gortel [33] following the earlier method by Heller [39], devised for the time-dependent wave-packet approach to semiclassical dynamics. This method requires solving for classical trajectories for classical variables according to eq. (6) and for quantum trajectories for quantum variables according first order quantum equations and finally, projects the results onto the desired energy surface.

Gadzuk model has the advantage of simplicity and can account for quantum effects like wave-packet squeezing or spreading, but it is valid only for harmonic potential where the wave-packet remains always Gaussian. For inharmonic potentials it can significantly deviate from the true quantum solution.

3.1.3 Beyond single excitation models or from DIET to DIMET

The common name of the presented models, that corresponds to the elementary 1D processes studied, is desorption induced by one electronic transition or DIET. These 1D models neglect the multi-dimensionality of polyatomic molecules desorption. For example, in the desorption of ammonia from metal surfaces, a large isotope effect was found that is not accounted for by the 1D models. Experiments have detected significant umbrella excitation in the desorbed ammonia and one must introduce the umbrella mode in treating the ammonia desorption. Thus desorption dynamics of

polyatomic molecules may involve several degrees of freedom. To this end, several multidimensional extensions have been reported [43,57,72,120-124]. Although computationally more demanding, the generalization to multidimensional space is formally straightforward. For this reason, we restrict this review mainly to 1D methods.

In the DIET models, if the time spent in the excited state is too short to ensure the gain of enough kinetic energy to desorb, then upon returning to the ground state the adsorbate cannot leave the surface. This particle will not contribute to the desorption yield in the DIET scheme. A generalization of DIET is DIMET, desorption induced by multiple electronic transition first advanced by Prybyla [9] then detailed by Misewich [40] and by Brandbyge [81]. In this scenario, a particle may be re-excited many times until it gains enough kinetic energy to desorb. The multiple electronic excitation allows accumulation of vibrational excitation on a timescale rapid as compared to vibrational relaxation typical of picoseconds order.

The DIMET model predicts relatively low kinetic energies of the desorbed particles and a desorption yield greater than anticipated for a simple DIET process. Also, DIMET leads to a nonlinear dependence of the yield on laser fluency as observed in all femtosecond desorption experiments, while DIET generally predicts a linear dependence.

The DIET model is most adequate to situations where nanosecond laser pulses are used. In this case, only a small concentration of hot carriers is produced and subsequent excitations of the molecule-surface bond are rare and therefore uncorrelated (the gain of vibrational energy is lost until another excitation might take place). The yield is linear with the fluency. On the contrary, when femtosecond laser pulses are used, the high intensity of the light produces a high-density of hot electrons that can excite in an additive manner the molecule-surface vibration leading to desorption. Then the DIMET model is the most adequate and the yield is nonlinear with the laser fluency. Other DIMET characteristics are that the desorbates are translationally and vibrationally hotter than in DIET and the translational and vibrational energy increase almost quasi-linearly with the fluency while they are fluency–independent in DIET case.

3.1.4 Perturbative treatment of desorption

Another wave packet quantum approach to explore the DIET and DIMET dynamics, developed following the same scenario as the Gadzuk model, was cast in terms of a time-dependent perturbation theory by Guo [41,42]. The system evolves according to the time-dependent Schrödinger equation:

$$i\hbar \frac{\partial \Psi}{\partial t} = H\Psi , \tag{7}$$

where H is the Hamiltonian of the system. This quantum dynamical calculation involves three stages: calculation of the initial wave function, solution of the evolution equation and final state analysis.

In a simple two-state model (the ground and the ionic one), the Hamiltonian can be written as follows:

$$H = h_g|g\rangle\langle g| + h_e|e\rangle\langle e| + h_{eg}|e\rangle\langle g| + h_{ge}|g\rangle\langle e| \tag{8}$$

where $|g\rangle, \langle e|$ represent the orthonormal neutral and ionic states of the system in the diabatic representation. The diagonal terms of the Hamiltonian are the sum of the kinetic and potential energy operators:

$$h_l = -\frac{\hbar^2}{2\mu}\frac{\partial^2}{\partial z^2} + V_l(z) , \text{ l=g,e,} \tag{9}$$

with μ the reduced mass and V_1 the corresponding potential. The off-diagonal elements represent the interaction between the two states due to the coupling with the electronic continuum of the substrate. If the system wave function is expanded in an electronic basis set, $\Psi = \psi_g |g\rangle + \psi_e |e\rangle$, the equation of motion for the nuclear wave packets reads as:

$$i\hbar \frac{\partial}{\partial t}\begin{pmatrix}\psi_e \\ \psi_g\end{pmatrix} = \begin{pmatrix}h_e & h_{eg} \\ h_{ge} & h_g\end{pmatrix}\begin{pmatrix}\psi_e \\ \psi_g\end{pmatrix}, \tag{10}$$

with the initial condition:

$$\begin{pmatrix}\psi_e \\ \psi_g\end{pmatrix}_{t=0} = \begin{pmatrix}0 \\ \psi_0\end{pmatrix}, \tag{11}$$

where ψ_0 is usually well defined as the eigen function of the ground state Hamiltonian.

The second-order time-dependent perturbation solution [42] of the evolution equation (10), corresponding to the typical, two-states MGR or Antoniewicz models, is analogous to a Raman process:

$$\psi_g^{(2)}(t) = -\frac{1}{\hbar^2}\int_{-\infty}^{t} dt' e^{-ih_g(t-t')/\hbar} h_{ge}(t') \int_{-\infty}^{t'} dt'' e^{-ih_e(t'-t'')/\hbar} h_{eg}(t'') e^{-ih_g t''/\hbar}\psi_0 \tag{12}$$

The second-order perturbative treatment presented above describes four coherent steps: excitation at t" from ground to excited state, propagation on the excited state for t'-t", deexcitation to the ground state at t' followed by propagation on the ground state to the time t. If in the above equation one replaces the off-diagonal elements h_{eg} , h_{ge} by delta pulses with a time delay τ: $h_{eg} = \hbar\delta(t''-0)$, $h_{ge} = \hbar\delta(t'-\tau)$, then one obtains the Gadzuk solution given previously (eq. (5), section 3.1.2). On the other hand, if one writes the coupling terms as: $h_{eg} = \hbar\delta(t''-0)$, $h_{ge} = \hbar f(q)e^{-\Gamma t}$, where Γ is related to the lifetime of the ionic state, one obtains the solution used in earlier papers on photodesorption, where an optical potential was introduced in the excited state to remove its population. In this case the Hamiltonian become non-hermitian. Obviously, the coupling terms describe the interaction with the substrate. Their magnitude is determined: directly by the substrate-adsorbate interaction and indirectly by the intensity of the optical pulses generating the hot electrons in the substrate. These coupling terms can also describe the dipole interaction with the incident photon [44]. In this case they depend on the electric field of the laser.

The framework discussed above, for the second order solution, represent the DIET limit where only a single excitation/de-excitation cycle is allowed and M=2. Higher order (M>2) solutions correspond to the DIMET case, where multiple excitation/de-excitation cycles take place in the presence of a strong laser field. The decay of the excited state complex is regarded as an incoherent process (analogous to the optical spontaneous emission). For DIET, the perturbation treatment is equivalent to wave packet evolution on the excited state under a modified Hamiltonian containing an imaginary optical potential i. e. $h_e' = h_e - i\Gamma(z)/2$ [43]. In the DIMET case, the non-linear fluence dependence of desorption yield comes out naturally [42]. The desorption probability of DIMET is proportional to the $2M^{th}$ power of the coupling strength that depends on the population of the hot substrate electrons. However, this population is not linearly related to the number of photons coherently absorbed by the substrate.

3.1.5 General time-dependent wave packet approach

The applicability of the perturbative model is reduced to low intensity laser pulses experiments. In high intensity experiments, the non-perturbative solution is obtained by propagation

of the Schrödinger equation (7). The method is independent on the number of implied states (two or more), the total wave function being decomposed on these states, so the method allows in principle multiple excitations. As in the preceding section, this quantum dynamical calculation involves three stages, construction of the initial state wave function, solution of the evolution equation and final state analysis. The initial wave function is calculated numerically as the ground vibrational eigenfunction of h_g. The evolution of the wave packet is obtained by repetitive application to the wave function of the evolution operator $e^{-iH\delta t/\hbar}$ written for the small time periods δt:

$$\Psi(t+\delta t) = e^{-iH\delta t/\hbar}\Psi(t) \tag{13}$$

The commonly used approximate propagation schemes are: the second-order difference method that uses a low order polynomial interpolation scheme, the interpolation based on the Chebyshev polynomial [45] and the split-operator technique (SO) [46]. In the SO method, the evolution operator is split symmetrically into the potential and the kinetic energy propagators:

$$e^{-iH\delta t/\hbar} = e^{-iV\delta t/2\hbar}e^{-iT\delta t/\hbar}e^{-iV\delta t/2\hbar} \tag{14}$$

The product of the three exponentials on the right hand side of the equation corresponds to an accuracy of order of $(\delta t)^3$. Each kinetic and potential energy operator application is carried out in a local representation. The potential operator V is local in the coordinate representation while the kinetic operator T is local in the momentum representation. Briefly, the numerical procedure consists of the following: (i) at each time step, the wave function $\Psi(z_i, t_j)$, discretized on a one-dimensional grid z_i, is multiplied by a phase factor $e^{-iV(z_i,t_i)\delta t/2\hbar}$, (ii) a fast Fourier transform is performed, yielding the wave function at discrete momentum grid points k_i, (iii) in momentum space the action of the operator $e^{-iT\delta t/\hbar}$ amounts to a multiplication with $e^{-i\hbar k_i^2\delta t/2\mu}$ at each grid point, thus it is not necessary to calculate any explicit derivatives, (iv) after switching back to coordinate space by an inverse Fourier transform, the second evolution operator containing the potential energy $e^{-iV(z_i,t_i)\delta t/2\hbar}$ is applied thus finishing the building of the evolution operator eq. (14). The propagation is norm conserving for a hermitian Hamiltonian [47], is stable and the time stability limit is independent of the δz, the spatial grid step mesh.

The desorption probability is obtained as the norm of the asymptotic wave function [42]:

$$P_{des}(t) = \int_0^\infty \left|\Psi_A(z,t)\right|^2 dz = \int_0^\infty \left|(1-g(z_a))\Psi(z,t)\right|^2 dz\,, \tag{15a}$$

or as the flux integral

$$P_{des}(t) = \int_0^t j(z_a,t)dt = \int_0^t \frac{i\hbar}{2\mu}\left[\Psi^*\frac{\partial\Psi}{\partial z} - \Psi\frac{\partial\Psi^*}{\partial z}\right]_{z=z_a} dt\,, \tag{15b}$$

where z_a is the analysis point and $g(z_a)$ is a cut-off function.

3.1.6 Multilevel wave packet methods

The standard two-states models neglect the continuum of the excited states of the metal and consequently, the interaction with the metal bath is difficult to introduce explicitly. Also the decay of the excited state is taken into account through coupling dependent on the resonance lifetime. The multiple state scheme allows to describe the decay of the ionic state through nonadiabatic coupling with a quasi-continuum set of electronic states. In the time-dependent framework, the nuclear motion on a diabatic potential energy curves can be written as [44]:

$$ih\frac{\partial}{\partial t}\begin{pmatrix} \langle e|\Psi\rangle \\ \langle g|\Psi\rangle \\ \langle c_1|\Psi\rangle \\ : \end{pmatrix} = \begin{pmatrix} h_e & h_{eg} & h_{ec_1} & : \\ h_{ge} & h_g & h_{gc_1} & : \\ h_{c_1e} & h_{c_1g} & h_{c_1} & : \\ : & : & : & : \end{pmatrix}\begin{pmatrix} \langle e|\Psi\rangle \\ \langle g|\Psi\rangle \\ \langle c_1|\Psi\rangle \\ : \end{pmatrix} \tag{16}$$

The off–diagonal elements contain the dipole interaction with the laser field and non-adiabatic couplings between the diabatic states. The later are responsible for the ultra fast quenching of the excited state of the adsorbate $|e\rangle$, quenching which is thus completely coherent. This idea was first advanced by Gortel [29,30] and was later used by others. Saalfrank [44], for example, uses nonadiabatic couplings having a lorentzian dependence on the desorption coordinate. Gaussian couplings where also used [48,49]. Recent calculations showed a decaying exponential dependence of the coupling functions on the desorption coordinate [50].

All these theoretical approaches are confronted with two basic problems: the microscopic modeling of the excitation and quenching processes, the proper inclusion of dissipation into the dynamic calculations. More concisely, these problems concern the quantitative interaction with the excited electronic bath. Although ample experimental data have been accumulated and the mechanisms of these processes have been extensively discussed, the detailed microscopic theories still lag behind. This is due to the large dimensionality and the complexity of the problem. For example, the explicit inclusion of both electronic and nuclear coordinates is very difficult. Even with the Born-Oppenheimer (BO) separation, reliable potential energy surfaces are scarce, even for the simplest systems. An attempt to go beyond BO was made by Harris et al. [51] that treated explicitly the coupling of the electronic motion in a photodesorption model through the transfer of an electron to the adsorbate. An effective model potential based on two coordinates, that of the excited electron contributing to the negative ion NO and that of the NO-surface distance is used to describe the time evolution of the wave packet until desorption occurs. The model includes automatically the non-adiabatic electron-adsorbate interaction. This approach is numerically time consuming because the large difference of masses between electrons and nuclei generates the need of very different time steps in the two degrees of freedom. It is also relatively inefficient because the nonadiabatic coupling is localized in a particular region where the potential energy curves are close to each other and has not to be introduced on the full two dimensional space.

3.2 Density matrix methods

Density matrix formulation of the time dependent problem of quantum physics allows a simple, rigorous treatment of systems that are open - the total energy of the system is not conserved, i.e. the dissipation of the energy of the system to a bath is taken into account. Before discussing these methods let us highlight how the wave function methods discussed above handle these classes of open systems.

One of the major points related to dissipation is the inclusion of the interaction between the electronic and nuclear degree of freedom through the nonadiabatic coupling. Most of the wave function approaches adopted a phenomenological electronic quenching rate obtained by fitting experimental observables. However the proper inclusion of the dissipation has also been tried in several ways. One of them, discussed above, is the simultaneous treatment, following Harris et al. [51], of the electronic and nuclei motions. Another is the use of imaginary potentials in the time-dependent wave propagation of two-states models [38,43,44].

As introduced above, in the density matrix theory of open systems, the adsorption complex is an open system where the total energy is not conserved. The excitation supplies energy to the system while the de-excitation dissipates energy to metallic electrons or transfer energy to a nuclei degree of freedom. The imbalance of the two processes provides desorbing energy to the adsorbate. According to Saalfrank [52], the density matrix description has the following advantages: (i) it is naturally applicable to thermal (mixed) states, (ii) it allows for an easy inclusion of energy exchange between the adsorbate-substrate system and the excited electronic bath (iii) it allows for the phase

exchange and the loss of the phase coherence between density on the upper and lower electronic energy surfaces due to many uncorrelated collisions of the hot carriers with the adsorbate-substrate complex.

As demonstrated by Blum [53], the time-evolution of an open quantum mechanical system cannot be described by the Liouville or Schrödinger equations. But, if the total system can be partitioned into a simple subsystem of experimental relevance and a bath, initially separable, then the dynamics of the open system is characterized in terms of the reduced density operator ρ that obeys the Liouville-von Neumann (LvN) equation:

$$\frac{\partial \rho}{\partial t} = L\rho = -\frac{i}{\hbar}[H, \rho] + L_D \rho . \tag{17}$$

Here L is the Liouvillian, H the Hamiltonian given by eq. (8) that describes the conservative dynamics of the system and L_D the dissipative Liouvillian that account for the interactions with the bath modes. The LvN equation is equivalent to the Schrodinger equation if the dissipative part is absent. The reduced density operator can be defined in an orthonormal, electronic basis that in the two-state [54-58] case reads:

$$\rho = \rho_{ee}|e\rangle\langle e| + \rho_{gg}|g\rangle\langle g| + \rho_{eg}|e\rangle\langle g| + \rho_{ge}|g\rangle\langle e| \tag{18}$$

with $\rho_{nm} = \langle n|\rho|m\rangle_{el}$ (n,m=g,e) being the elements of the density operator. The diagonal matrix elements ρ_{mm} are interpreted as the population of the states while the off-diagonal matrix elements ρ_{nm} are a measure of the phase coherence between the states n and m and are responsible for interference effects.

The dissipative Liouvillian is often calculated in the Markov approximation. This approximation states that at time t, $\rho(t,t') \cong \rho(t)$, i.e. $\rho(t)$ loses the memory of all the past events t'. The Markov approximation is justified for fast relaxation to the bath as, for example, the hot-electrons mediated processes. Even in this case the choice of L_D is not unique. In the Redfield-type theories the operator L_D is derived from microscopic Hamiltonian but then the elements of the density matrix can become negative and loose their interpretation as probabilities. In the phenomenological approach of the dynamical semigroup formalism of Lindblad [59], L_D is defined as:

$$L_D \rho = \sum_k (\hat{C}_k \rho \hat{C}_k^+ - \frac{1}{2}\left[\hat{C}_k^+ \hat{C}_k, \rho\right]_+) \ , \tag{19}$$

where the elements of the density matrix are always positive and $[\ldots]_+$ is an anticomutator. Here $\hat{C}_k$ are Lindblad operators that determine the dissipation nature and the relaxation speed, while k labels vibrational and electronic relaxation, pure electronic or vibrational dephasing or phase fluctuations in an external electromagnetic field channels. Some simple form of Linblad operators will be given below in connection to NO/Pt desorption.

The formal solution of the Liouville-von Neumann equation is given by:

$$\rho(t) = e^{Lt}\rho(0) . \tag{20}$$

As for the wave packet methods, there are various ways to approximate the evolution operator in a numerical application. The simplest solution is to diagonalize the Liouvillian and use its eigenvalues to construct the propagator. This approach is sometimes instable because the Liouvillian is a complex, non-symmetric, often ill-conditioned operator [60]. Other methods that do not require diagonalization are (i) the Runge-Kutta method, (ii) split superoperator [61,62], (iii)

polynomial interpolation schemes [63-66] using Newton [64], Faber [65] or Chebyshev [66] polynomials. The evaluation of the operation Lρ needs the choice of a representation. All operators are represented on a grid of evenly spaced points and the commutators or anticommutators from eq. (17) or (19) are evaluated locally i.e. in a representation where the operators are diagonal. The time propagation is performed dividing the time interval in steps δt, small enough to resolve variations in the operators, and the evolution operator is calculated at each step. The reader is referred to the work of Berman *et al*. [64] for further details. Finally, the expectation values of quantum mechanical operators A, of the property of interest, are calculated by taking the trace in the electronic matrix, evaluated in the configuration space representation:

$$\left\langle \hat{A} \right\rangle (t) = tr\left\{ \hat{A}\hat{\rho}(t) \right\}. \tag{21}$$

In the models describing the NO/Pt desorption [52,54-58,114,115] were used the above formulation in terms of the Liouville-von Neumann equations and the electronic quenching in terms of the Linblad dynamical semigroup approach. Within this formalism, the direct excitation by photons and indirect excitation by hot electrons in both DIET and DIMET limits were treated.

For DIET dynamics, one starts from the excited state, $\hat{\rho}(0) = \hat{\sigma}\left| e \right\rangle\left\langle e \right|$, where $\hat{\sigma}$ is the ground state density operator, derived from the vibrational states of V_0. The nuclear density evolves on the excited state potential and may be transferred on the ground state through quenching. This quenching represents here the coupling of the excited absorbate with the metal electronic excitation and is modeled through a single Linblad operator $\hat{C}_1 = \sqrt{\hat{\Gamma}_{ge}}\left| g \right\rangle\left\langle e \right|$, $\hat{\Gamma}_{ge}$ being a rate operator that can be also coordinate-dependent because the electron tunneling probability decays exponentially from the surface.

For DIMET dynamics, the adsorbate is in its electronic ground state, $\hat{\rho}(0) = \hat{\sigma}\left| g \right\rangle\left\langle g \right|$. The indirect excitation step is explicitly included and modeled by a Linblad operator $\hat{C}_2$ of the form $\hat{C}_2 = \sqrt{\hat{\Gamma}}_{eg}(t)\left| e \right\rangle\left\langle g \right|$. The rate $\hat{\Gamma}_{eg}$ is time and coordinate dependent and is related to the quenching rate through the principle of detailed balance $\hat{\Gamma}_{eg}(z,t) = \hat{\Gamma}_{ge}(z) \cdot \exp\left\{ -\frac{V_{-}(z) - V_0(z)}{k_b T_{el}(t)} \right\}$, where $T_{el}(t)$ is the temperature of the metal electron gas calculated within a coupled diffusion model (CDM) [67].

In the aforementioned methods, the calculation of the dissipation term that includes the hot electron dynamics is still an open question. The hot electrons energy distribution is considered to be the Fermi-Dirac distribution function even in these far from equilibrium conditions. This distribution is related to an electronic temperature calculated using CDM. The photodesorption yield was found to vary nonlinearly with the electronic peak temperature. One can obtain a nonlinear dependence of the yield with the laser fluence only by assuming a linear dependence of this electronic peak temperature on the laser fluence. However, such temperature/fluence dependence was not yet demonstrated. The CDM model considers the metal composed by two subsystems, electrons and phonons. Each subsystem is supposed to be in a local equilibrium corresponding to an effective temperature. But experimental results [97,98] show that in the sub-picosecond regime the distribution function has a form different from the Fermi-Dirac distribution function. Moreover, the system returns to equilibrium conditions in a time longer than the desorption time of less than 1 ps. Therefore one can not correctly describe the present non-equilibrium electrons using a function based upon a temperature or the transitions rates that are function of such a temperature.

A different approach to desorption using again the density matrix formalism was developed by Micha [68,69]. The Hamiltonian of the extended molecular system is divided into a term for the localized primary degree of freedom (DFs) affected by desorption and treated by the Liouville-von Neumann equation for the density operator. These primary DFs are coupled to the secondary DFs that act as a bath and are treated through a stochastic theory of localized perturbations in an extended system. A self consistent field treatment gives an effective non-hermitian Hamiltonian for the

primary DFs that accounts for energy fluctuation and dissipation. The bath dynamics is studied when secondary DFs are either lattice vibrations or electronic excitations.

Another approach for laser induced desorption is the vibrational-heating mechanism (VHM) developed by Gao [70,71]. In this model, the fast energy transfer between the electron bath and the adsorbate-surface vibration leads to heating and breaking of the local bond in the femtosecond scale range. Starting from the Liouville-von Neumann formalism for the density matrix, a general kinetic equation is derived for the reduced density matrix distribution. In the eigenstate representation, the diagonal approximation of this equation corresponds to the generalized Pauli master equation, while the off diagonal part describes the quantum coherence beyond the master equation. For a bond with no initial coherence and weak electron-vibration coupling, the effect of the off diagonal elements is negligible. The formalism was applied successfully to desorption of O_2 from a Pt(111) surface, obtaining a nonlinear yield-fluence dependence [71].

The numerical efficiency of the density matrix is lower than that of the wave packet methods. If N is the number of grid points in one dimension, the evaluation of the Hamiltonian operation scales as $N^2 \log N$ in density matrix compared to $N \log N$ in wave-packet methods. This is the principal drawback of the density matrix methods. As shown numerically and semi-analitically by Saalfrank [54,58], one can devise methods, based on stochastic wave packets (i.e. by repeated solutions of Schrödinger equation with non-hermitian Hamiltonians) that in some cases are memory saving alternative to density matrix propagation schemes. One example is the Monte Carlo Wave packet method (MCWP) where the propagation of the wave packet is performed using a non hermitian Hamiltonian that includes dissipation as an imaginary potential. In that model the wave packet passes from a potential curve to another by arbitrary quantum jumps. After analyzing the loss of the norm (due to a temperature dependent term) by comparing it to a random number, the MCWP algorithm eventually renormalizes the wave function. The yield is obtained by averaging over several calculations. The equivalence between a density matrix method and MCWP is valid only for a dissipative part of a Linblad form (DIET) and not too low desorption probability. For DIMET processes, the presence of the excitation term in the Hamiltonian leads in the MCWP to re-excitation of the quenched trajectories and the convergence is much harder to attain. Also, for coordinate-independent quenching rates, Gadzuk's weighted average procedure [54] is a rapidly converging variant of the stochastic wave packet approach, and therefore rigorously equivalent to the exact solution of the Liouville-von Neumann equation. However, Gadzuk's scheme is not generally applicable to multiple dissipative channels, coordinate-dependent quenching, direct and indirect excitations and to multiple excitations- deexcitations processes.

3.3 Time-independent methods

The time-independent methods discussed here follow the terminology used in the original papers by Seideman et al. [72,73]. The title comes from the use of a set of time independent basis functions in the expansion of the wave function:

$$\Psi(t) = \sum_l \sum_{j_l} C_{j_l} \left| j_l \right\rangle e^{-iE_{j_l}t} + \sum_n \int dE C_{E,n}(t) \left| E, n^- \right\rangle e^{-iEt}, \tag{22}$$

and only the expansion coefficients are time dependent. Here $\left| j_l \right\rangle$ (l=g, e) denotes the bond and/or quasibond states of the zero order Hamiltonians h_l, given by eq. (9), and $\left| E, n^- \right\rangle$ the incoming-waves scattering states of the ground state Hamiltonian h_g.

This time-independent approach is an alternative to the time-dependent one. It will provide a complementary insight and serve to enhance the general understanding of DIET or DIMET, offering closed form expressions for the observables of interest. The time-dependent approach describes well and is efficient for rapid processes, particularly when the operators themselves are time dependent and desorption is essentially one-dimensional. Its use is advantageous when desorption process proceeds via excitation of internal modes, involving long-time dynamics on the ground PES due to the presence of pre-desorbed states. In this last case of the long-time dynamics, instabilities can

appear in the usual time-dependent approaches (subsections 3.1.2-3.1.6). Also, the outcome becomes sensible to the cutoff distance separating the internal and the asymptotic region.

Here, we briefly present this time-independent methodology, the reader is referred to the original papers of Seideman et al. [72,73] for details and applications. In the two-states approximation, the system Hamiltonian is given by:

$$H = H_0(q) + H_{\text{int}}(q,t)\,, \tag{23}$$

where q denotes collectively the nuclear coordinates. Born-Oppenheimer approximation is assumed and the electronic coordinates have been integrated out. H_0 is the Hamiltonian of the two uncoupled electronic states, represented by the diagonal terms h_g and h_e given in eq. (9). H_{int} induces a population transfer between the two electronic states and energy transfer between the system and the environment,

$$H_{\text{int}}(q,t) = V_{ex}(q,t) + V_{re}(q,t)\,, \tag{24}$$

where V_{ex} has the effect of building up and V_{re} the effect of depleting excited state population. In short-pulse, high intensity experiments, the interaction is non-perturbative and generates a large amount of hot-electrons. In that case, V_{ex} models the time-dependent electronic occupancy and is taken dependent by the electronic temperature $T_{el}(t)$, determined by CDM:

$$V_{ex}(t) = \frac{v_{ex}(q)}{1+\exp\left\{\left[V_e(q) - V_g(q)\right]/k_b T_{el}(t)\right\}}, \tag{25}$$

where V_l, (l=g, e) is the potential of the ground and the excited states and $v_{ex}(q)$ is a system-dependent function; V_{ex}, V_{re} are related through microscopic reversibility.

Subsequent to the external excitation, the complete wave function is given in Eq. (22) as a superposition of ground and excited levels. Substituting the Hamiltonian and the wave function in the time-dependent Schrödinger equation and using the orthonormality of the states one obtain a set of coupled differential equations for the developing coefficients $\{C_l\}$ and $\{C_{E,n}\}$. Time propagation of these equations is formally equivalent to solving the Schrödinger equation.

The probability of observing photodesorbed molecules in an asymptotic state n, at total energy E (state that is considered as desorbed) is $P_n^{des}(E,n) = \left|\langle E,n|\Psi(t)\rangle\right|^2 = \left|C_{E,n}(t)\right|^2$ so that, the direct component of desorption probability is given by: $P_D^{des}(E,t) = \sum_n \left|C_{E,n}(t)\right|^2$, which, integrated over the energy, gives the time-resolved direct component of the desorption probability, the complete desorption probability for a fast nuclear dynamics. For an indirect, resonance mediated desorption process the direct component is supplemented by a resonant component dependent on the vibrational relaxation rate. Desorption of ammonia from a copper surface, where the process is determined essentially by vibrational relaxation and decay to the continuum, was studied within this method as well as desorption of NO/Pd that is dominated by a high concentration of hot carriers.

3.4 Classical dynamics methods

Classical trajectory methods assume that the nuclear motion is governed by the Newton mechanics. They can be used to study large systems where a quantum treatment is not tractable particularly in molecule-surface scattering and gas-phase dissociation. They are reliable for fast, direct processes involving high energies and large masses, but fails to describes tunneling dynamics or resonances.

In a classical dynamical calculation, the same steps as in the quantum methods above should be followed: the choice of initial conditions, the propagation and the final state analysis. The initial

conditions, i.e. the initial positions and momenta, are determined by the initial parameters such as the translational energy, angular momentum internal state quantum number etc. These parameters may be derived from the ground state wave function [75-77]. The propagation is done using numerical integrators to solve the classical Hamilton's equations (6) and a trajectory is considered terminated when a set of criteria are satisfied. From the final state distribution one extracts usually the desorption yield, the translational and internal-state distribution.

The classical trajectory methods assume usually the validity of the Born-Oppenheimer approximation (BOA). Breakdown of the BOA does not necessarily mean that the nuclear motion is not classical but rather that the classical motion occurs on two or more PES connected by a hopping from one surface to another, the probability being given by the non-adiabatic coupling. DIET and DIMET models can be treated classically within such a hopping scheme. For example, using a classical hopping within the DIET model, Hasselbrink [77] described the coupling of the rotational and translational degrees of freedom of NO/NiO system whereas, using DIMET model, Misewich et al. [40] studied the NO/Pt(111)system.

In these approaches the substrate excitation and the role of the hot electrons is only roughly taken into account by the hopping probability. A different model in the classical framework is the molecular dynamics with electronic friction (MDEF) [78-80]. The MDEF model considers that the nuclear motion takes place on a continuum of potential energy surfaces of a metal and the nonadiabatic energy exchange between nuclear and electronic degrees of freedom is included through an electronic friction force. In this situation BO approximation fails since for any motion of atoms of the adsorbate, such as vibrations, rotations and translations, there are resonant electronic excitation of the metal. Such excitations are highly delocalized, so the continuum of electronic potential energy surfaces are similar and can be replaced by a single, effective PES [80]. The working equations for the nuclear degrees of freedom are those of classical molecular dynamics with the addition of a friction term describing the nonadiabatic energy transfer from the nuclear to electronic excitations and a fluctuating force for the reverse process to fulfill the energy balance

$$m_r \ddot{r} = -\frac{\partial V}{\partial r} - \sum_s K_{rs}\dot{s} + R_r(t) \ . \tag{26}$$

Here, V is an effective adiabatic PES, K_{rs} and $R_r(t)$ are the friction kernel and the random force. This equation is known as Langevin equation initially devised for the study of the Brownian motion. This equation can be thought of as arising from frequent low energy electronic transitions between a continuum of nearly parallel potential energy surfaces. The rapidity of these transitions relative to nuclear motion permits their representation as friction and random forces with no explicit electronic dynamics involving. The electronic friction can be obtained using molecular orbital calculations. In the Markov limit, when memory effects are neglected, the random forces can be evaluated using the fluctuation-dissipation theorem between friction and fluctuation forces [74], via an effective electronic temperature T obtained using CDM [78,79]:

$$\left\langle R_r(t) R_s(t=0) \right\rangle = kTK_{rs}\delta(t) \ . \tag{27}$$

MDEF simulations of laser induced desorption for CO/Cu, where the energy given by the laser is included through the temperature T in the fluctuating force $R_r(t)$ of eqs. (26), (27), were performed [78,79].

DIET and DIMET models are diabatic pictures of the desorption process in which the potential energy surfaces (PES) are coupled through a hoping between the PES. The DIMET picture is able to take into account the transition between ground and excited states of the adsorbate but it cannot describe the electronic friction. The MDEF picture in its classical form cannot describe the highly excited electronic (ionized) states of the adsorbate. A unified picture of energy transfer from excited 'hot' electronic states, both of low energy (friction like description) and high energy (DIMET-like description) was given by Brandbyge [81]. The adsorbate is modeled as having a single electronic level ε_a that can tunnel into the continuum represented by the metal conduction band giving it a lifetime broadening Δ. One can distinguish two situations. First, if the width Δ is large (the lifetime is short) and of the same order as the energy difference between the energy

maximum of the resonance and the Fermi level E_F, then there is no energy gap. In solid state theory this situation corresponds to a single band where the primary excitation leads to the electron-hole pairs formation. Formally, the mechanism can be described through a temperature independent friction force. Now, if the width Δ of the adsorbate resonance is narrow (the lifetime is large) relative to the maximum of the resonance energy measured from the Fermi level E_F as well as to the width of the conduction band, then the mechanism can be described as in DIMET scheme where multiple excitations between two distinct levels living long enough appear.

4. Application. CO desorption

The methods described above were applied extensively to study the photodesorption of some prototypical adsorbates, as for example NO, NH_3 and CO adsorbed on metal or oxide surfaces. NO is a probe molecule for studying the dynamics of molecule-surface interaction because it is easily excited and one can measure the fluorescence spectra, signature of its internal energy distribution. NH_3 molecule has been also largely investigated because of the role played by an internal degree of freedom in the multi-dimensional desorption. The reviews of Zhou, Zhu and White [5], Zimmerman and Ho [6] and Guo, Saalfrank and Seideman [8] examined in detail the literature published on the NO and NH_3 desorption and the reader is referred to their work for detailed information. In the present review we will concentrate only on CO desorption from metal surfaces that have received less attention despite the amount of work carried out by various research groups [2,3,15-18,49,50,68-71,75,76, 78-80,82-89, 91-95,99-102,106,109].

Non-thermal desorption of CO was obtained from W [86], Ru [3], Pt [16-18], Cu [2,15] and also from oxidized Ni [82-84] or Cr_2O_3 [85] but for Ni surface the desorption yield was negligibly small. ESD [87,88] and STM [89] have also been reported. In most of these experiments, not only the integral desorption yield and translational energy were measured but also state-resolved data such as the vibrational and rotational population.

CO/Cu is a system rather well investigated both experimentally and theoretically. Over the other systems, it has the following advantages: at low coverage the CO molecules stay mainly in on-top position on Cu(111) and Cu(100) surfaces, making the system appropriate for 1D study; CO is a stable molecule on nearly all metals so the desorption process do not interfere with the dissociation; the bonding CO-Cu is weak, being at the limit between physisorption and chemisorption, being interesting for catalytic modeling. Such systems allow adsorption and desorption at low energy expense thus facilitating the reactions at metallic surfaces [90] and corresponding to prototype reactions.

In a first experiment performed on CO on Cu(111), Prybyla et al. [2] reported a very fast desorption process, less than 325 fs, measured with Second Harmonic Generation (SHG) method, after irradiation with 100 fs, 2 eV laser pulses. The quantum efficiency was of about 10^{-3} per absorbed photon, much higher than observed for other molecule/metal systems. The desorption yield, measured by a mass spectrometer increases nonlinearly with the laser fluence by the power law $F^{3.7}$. Desorption of CO from Cu(100) was later investigated by Struck et al. [15] with a 160 fs, 3.1 eV laser pulse obtaining a yield dependence of $F^{8\pm1}$ and a 3 ps desorption time measured by a pump/probe experimental set-up. The kinetic energy distribution of fragments was deduced from the time-of-flight spectra. The average kinetic energy was 0.037 eV, giving a flux-weighted translational temperature of T_{kin}=215 K. The rotation was only slightly excited, T_{rot}=225 K, while the vibrational temperature was of T_{vib}=1330 K. These results depend on the laser fluence, increasing slightly with the fluence increase. We note that the difference between these two experiments is significant. The huge difference between the two desorption times can be actually explained. The SHG method of Prybyla [2] measures in fact the polarisability of the surface atoms and is sensitive to the CO coverage; the signal increases with the diminishing CO coverage and stabilizes at a constant value afterward. The time needed to attain the constant plateau value was identified to correspond to the duration of the desorption event. The SHG time, measured by Prybyla et al., should be considered as a lower limit of the desorption time, because, to be counted as photodesorbed, the molecules should leave the interaction region. In the experiment of Struck et al. [15], the pump laser was split into two beams orthogonally polarized and applied normal to the surface. Information about the desorption

time was obtained from two-pulse correlation data. The desorption yield as a function of pulse/pulse delay time was found to be of a Gaussian shape with a FWHM of about 3 ps. But this set-up only proves the nonlinearity of desorption with the absorbed laser fluence and the existence of a finite time for desorption. The width of the Gaussian function cannot be considered as the actual desorption time but only as an upper limit of the response time of the system. One cannot explain the differences between the power laws mentioned above by the experimental conditions or the surface cut. Precisely, the structure of the surface of the metal, e.g. the presence of a surface state on Cu(111) but not on Cu(100), the position symmetry of the adsorbate on the surface or the difference in the energy, fluence or duration of the two lasers can not explain such a huge difference in the power law. In fact this large discrepancy in the yield behavior raises several questions, for example, about at least the way the fluences were measured in the two experiments.

MDEF simulations of femtosecond laser induced desorption of CO/Cu(100) were performed at zero coverage limit [78] and for saturation coverage [79]. The gas-surface interaction potential is calculated for a single CO molecule interacting with a slab of 6x6x3 Cu atoms, being a sum of atom-atom contributions from C-Cu, O-Cu and O-C. The parameters were chosen to reproduce binding site properties at equilibrium geometry [91]. Saturation simulations include additionally gas-gas interaction potential sum of van der Waals terms and electrostatic interactions approximated as quadrupole-quadrupole (the dipole momentum of the molecule is virtually zero). The qualitative dependence of the desorption yield on laser fluency, and the underlying desorption mechanism are similar at low and high coverage. In each case, the results show a substantial selectivity in the nature of the nonadiabatic or electron-hole energy flow, materialized in the friction Kernel K_{rs}. This selectivity is leading to a major transfer of that energy to the frustrated rotation instead of the normal vibration degrees of freedom. If the friction kernel K_{rs} do not contain in-plain degrees of freedom then the desorption yield diminishes to virtually zero, while deleting the normal degrees of freedom has only a minor effect on the yield. The preference for a “cartwheeling” desorption mechanism (rotation angular momentum parallel to the surface plane) versus vertical desorption is consistent with the strong nonadiabatic coupling between the in-plane frustrated rotation mode and substrate electron-hole pairs relative to weak or no coupling with the normal frustrated translation mode. Moreover a transfer among certain phonon modes also occurs. For example, for CO/Cu(100) [80], the characteristic energy of the hindered rotation (282 cm^{-1}) is close to CO-surface vibration (305 cm^{-1}) but very different from C-O stretching (2102 cm^{-1}) and frustrated translation (24 cm^{-1}). Because of the very close vibrational quanta, energy interchange between rotation and CO-surface vibration is very efficient and can lead to desorption. This interaction can also explain why CO molecules desorb rotationally less excited than vibrationally.

The desorption yield depends nonlinearly on the laser fluence ($Y \sim F^{5.3}$ versus $Y \sim F^{5.6}$ at saturation) but there is a significant enhancement of the total desorption yield at saturation relative to the zero coverage limit. This is due to the increased corrugation of the potential in the presence of neighboring adsorbate molecules in addition to the energy pooling between adsorbate molecules in the overlayer. It is interesting that some molecules may acquire energy only due to the cumulative/cooperative inelastic collision with the neighboring molecules. This is a type of dynamics that has not been explicitly considered in other papers. Variation of the corrugation at desorption (the change of in-plane momentum to normal momentum that appears here in collision of the adsorbates with their neighbor in the overlayer) was also put in evidence on sticking at surfaces [92-94]. Experiments performed on NO/Pt [94], CO/Ni [93] and classical trajectory simulations on CO/Cu(100) [92] showed also a variation of the corrugation with the value of the incident energy. Less energetic molecules have time to adjust to its minimum energy orientation and the corrugation is small whereas, at higher energies, the reorientation has much less time, resulting in increased corrugation.

Classical trajectory approach and quantum wave packet propagation performed [75,76] for CO physisorbed on nonmetallic surfaces showed that the degree of excitation of frustrated rotation plays a crucial role in desorption. The degree of initial vibrational excitation has much less effect on the probability of desorption. Also inclusion of the hindered translation lowers the frustrated rotation threshold. These results prove that direct coupling between stretching or translation with frustrated rotation is weak, while energy exchange between rotation and CO-surface vibration is very efficient and can lead to desorption. These results are in agreement with the characteristic frequencies of the

different motions. CO desorption from oxidized surfaces like NiO [82-84] or Cr_2O_7 [85] depends also on the frustrated rotation. For example, desorption from NiO is characterized by a bimodal rotational distribution that may suggest the presence of two adsorption species, one with the molecular axis perpendicular to the surface, which results in a "cold" rotational distribution and a tilted geometry, which leads to rotationally "hot" desorbing molecules. On the contrary, as CO molecule adsorbed on Cr_2O_7 is oriented parallel to the surface, the desorption of CO have to be monomodal. Experiments showed that is really the case.

A density matrix theory has been developed by Micha et al. [68-69] for indirect photodesorption of CO from Cu(001) surface, where a local electromagnetic field in the substrate induces an effective primary dipole. The system was separated into a primary region formed by the adsorbate and the bonding substrate and a secondary region including the remaining substrate strongly coupled and interacting. The authors demonstrate that the dynamics of the primary region is governed by an effective Hamiltonian which includes dissipation and can be derived under the assumption that the secondary region undergoes stochastic motions over which is possible to average primary quantities. The PES of $(Cu)_n$-CO clusters were calculated using semi-empirical electronic energy program, in the ZINDO approximation, giving the ground and the excited PES and the transition dipoles of CO/Cu system. An analysis of the ground and excited states shows the occurrence of an electronic rearrangement during excitation but does not indicate the capture of the electron by the CO as is specified by the Gadzuk model. The dynamics of desorption was assumed to involve the frustrated translation. The desorption probability was calculated using the wave packet propagation. In a first attempt, the effective primary dipole moment was calculated by applying the perturbation theory to find the response of the secondary region to the local field that couples, through Coulomb interaction, to the primary region. The resulting yield was nearly proportional to the laser fluence as would be expected from the first order perturbation theory. Then a more involved calculation was performed to obtain a primary dipole that results in a dipole directly dependent on the laser fluency ($D \sim F^n$). In that case, desorption yield depend nonlinearly on the fluency.

The vibrational heating mechanism (VHM) of Gao et al. [70,71] has been applied to the CO/Cu(100) system. For simplicity reason, a one-dimensional harmonic oscillator truncated at one side of the potential wall, at the energy corresponding to bond breaking, is adopted to represent the desorption coordinate. This model can be misleading from the kinetic point of view because accumulation of vibrational energy involves climbing up a progressively softer potential but it contains the qualitative features of the reaction dynamics [119]. The distribution of hot electron at the surface is approximated by that of a homogeneus gas with a time dependent temperature fulfilling a Gaussian law. Electron-adsorbate interaction is described by resonant coupling via an unoccupied resonance of the adsorbate. Due to the multiple electronic transitions giving rise to the vibrational heating, the model is analogous to DIMET. The dynamics of the oscillator under multiple electronic transitions is described by a density matrix, spanned over the oscillator states, the evolution of these states being governed by the Pauli master equation. The sub picosecond response of the vibrational distribution, essential in bond-breaking by femtosecond lasers, is found to be non-thermal and the probability of multiple excitation is much higher than that given by the classical limit. The model was successfully applied to the desorption of O_2/Pt(111), but it failed in the case of CO photodesorption from Cu(100). A slightly modified model has been successful in describing desorption of CO from Cu(111) induced by electron inelastic tunneling originating from a STM [95]. In this case, non-equilibrium heating, between the C-O stretch and CO-Cu vibration, occurs due to different coupling strength between the electrons resonances and phonon motions. Inharmonic coupling between two phonon modes, highly excited stretch to the cooler molecule-surface bond, leads to energy transfer and drastically influences the bond-breaking process at the surface.

The interpretation of the STM experiments by Bartels et al. [89] was made using the above model. These authors identified the underlying process as occurring through an intermediate resonance of CO $2\pi^*$ orbital, having a lifetime of 0.8-5 fs. To describe the dynamics of STM induced desorption of CO from Cu(111), a microscopic theory [96] based on the CO $2\pi^*$ excitation was also proposed. In this theory, a single electron initially occupies the CO $2\pi^*$ orbital. Excitation of the CO-Cu vibration, described by a Morse potential, then occurs and the electron tunnels from the $2\pi^*$

orbital to the metal. This mechanism allows climbing the vibrational levels of the CO-Cu bond up to an unbound level and CO desorbs from Cu. The probability of finding the electron in the CO $2\pi^*$ orbital and the CO desorption rates were obtained by solving the master equation. By adjusting some parameters, Hasegawa et al. [96] were able to reproduce an experimentally observed ultra-low desorption yield.

The panorama of desorption models described above showed that there are many physical ideas of how the energy is concentrated in the photodesorption mode allowing bond breaking. But a calculation of the dissipation term taking into account the non-thermal character of the process is still missing particularly because the desorption is faster than 1 ps. In many of the models presented above, the influence of the hot electrons was introduced only through an effective electronic temperature obtained using CDM [67]. As already explained this model considers the metal composed by two subsystems, electrons and phonons. Each subsystem is supposed to be in a local equilibrium having an effective temperature defined through a distribution function, Fermi-Dirac for the electrons and Bose-Einstein for the nuclei. But in the sub-picosecond regime the electrons are far from equilibrium, the distribution function has a form different from the Fermi-Dirac one and no temperature can be defined. However, in the models presented above the nonlinear yield with the laser fluency can be obtained only if the temperature is included.

In a recent paper [49] we tried to obtain the non-linear yield-fluency behavior through an optical potential dependent on the hot electron population and showed that is one of the possible ways allowing to withdraw the assumption of an electronic temperature. Precisely, we proposed a 1D model for photodesorption involving three-electronic states. The associated mechanism of desorption closely follows the ideas of Gadzuk, but we used three diabatic electronic states coupled by an electrostatic interaction. The laser excitation is indirect, acting only on the substrate. Two of the electronic states correspond to the neutral adsorbate bonded to the excited substrate (the metal electrons are excited at different energies) and one state corresponds to the negative ion of the adsorbate bonded to the unexcited metal. The ground state was constructed much in the same way as in the MDEF simulations [91], except that we used a slab of 16x16x3 Cu atoms. The excited state potential was first verified, by ab initio calculation, to correspond to a charge transfer, then four charge-charge image terms were added to the ground state potential. The electrostatic (non Born-Oppenheimer type) interaction, taken of the form of a Gaussian function, was localized near the curve crossing and determines the electron hopping between states. To include the hot electrons of the metal in our model, we added an optical (interaction) potential in the Schrödinger equation that acts as a population provider. It is constructed much in the same manner as our non-equilibrium distribution function [99], with an excitation and a de-excitation term. However, in this paper we tried to take into account, in an effective way, the interaction neglected in the earlier kinetic model, such as: secondary electrons, electron-phonons collisions and electron-surface state interaction. Within this model [49], we obtained by wave packet propagation (see 3.1.6) a yield dependence of the form $Y \sim F^{4.5}$ and a kinetic energy distribution quite comparable with the experimental one.

In order to see the interplay between direct and indirect excitations of the CO $2\pi^*$ resonance in the CO desorption from copper surface, put on evidence by STM [89] and two-photon photoemission experiments (2PPE) [100], we developed comparatively a two-states conservative system model and a three-states non-conservative, open system, model [50]. In both models, the Hamiltonian includes the band structure of the surface, the laser-matter interaction and the non-adiabatic couplings where the last two terms are function of the desorption coordinate. The two-states model includes the ground and the ionic state and only the direct laser excitation of the negative ion resonance. In the three-states model, a third, excited state is added. The presence of this state allows inclusion of the direct and indirect laser excitations. The open character of the system appears through (i) a dephasing between excitation and de-excitation events (ii) a phenomenological quenching rate of the third state. At each fluency, the desorption probability is calculated for a sampling of dephasings and the yield is obtained as an average over these desorption probabilities. Compared to the standard, conservative two-states model, the open three-states model displays a Gaussian distribution of the desorption probability with the dephasing, indicating the random character of incoherent processes and a nonlinear photodesorption yield with the laser fluency. The results of the three-states model can be adjusted to be in agreement with the experimental yield. Here we obtain $Y \sim F^{4.9}$ for the chosen three independent parameters.

Recently, we demonstrated that, for surface problems, one should use spatially dependent laser-matter interaction working with the potential vector $\vec{A}(\vec{r})$, respectively the $\vec{A}\cdot\vec{p}$ gauge in the Hamiltonian [101]. The laser-matter interaction was generally described in the dipole approximation (called $\vec{E}\cdot\vec{d}$ gauge), considering that $\vec{E}$ would not vary spatially at the gas-solid interface due to the long wavelength. However, due to the sudden jump of the electron density at the gas-solid interface, the electric field is spatially dependent, and the dipole approximation is no longer valid. In order to quantify the difference between the two gauges ($\vec{A}\cdot\vec{p}$ and $\vec{E}\cdot\vec{d}$), we developed a two-states desorption model for these two gauges, including the direct excitation of the negative ion resonance by the laser [102]. The interaction terms, parametrically dependent on desorption coordinate, were calculated using electronic wave functions optimized for the surface structure. For the two gauges, the yield displays the same shape but is quantitatively different and the result strongly depends on the laser polarization. Experiments showed that desorption [103] or 2PPE data [104] can be strongly dependent on the laser beam polarization.

Electron stimulated desorption of CO chemisorbed on Ru(001) surface was easily obtained [87,88] and showed similar translational, rotational and vibrational distribution as the CO/Pt(111) system. Recently, Funk et al. [3] obtained CO desorption from Ru(001), using a 800 nm, 130 fs laser of fluence between 100 and 380 J/m^2, almost six time greater than the largest fluency used in other desorption experiments (60 J/m^2). The desorption yield was nonlinear with the laser fluence fulfilling a power law ~F$^{4.5}$ and the two-pulse correlation measurements revealed a response time of 20 ps. These results may qualitatively be reproduced using the empirical friction model proposed by Brandbyge [81]. The very long desorption time, the sharp rise of the calculated phonons temperature and the specific electronic structure of the CO/Ru system strongly indicate a phonon mediated process.

A remarkable case is CO on Pt surfaces where desorption was obtained with femtosecond pulses [18] CO/Pt(111) as well as with nanosecond pulses [16,17], for CO/Pt(001) thus differing from other metals where desorption was obtained only with short pulses of femtosecond duration. In the ns scale the laser intensity is 10^{-4} lower than in the fs scale, so one expect a desorption more like DIET then DIMET and consequently a linear yield. However, desorption from Pt(001) at 193 nm (6.43 eV), 6 ns showed a nonlinear yield versus fluence behavior and desorption of two species: CO and CO^+. The yield exhibits a F^3 and F$^{1.8}$ dependence on fluency for CO and respectively CO^+. For CO desorption, a mechanism of desorption by three-photon ionization, leading to a temporary positive adion, followed by neutralization was proposed. CO^+ desorption results from two-photon electronic excitation of the ad-molecule followed by its ionization due to the transfer of an electron to the metal. As in the CO/Cu case, the desorbed molecules were rotationally cold but vibrationally hot, even if the intermediate state was different in the two cases (a positive ion, not the negative one). Recent experiments [18] performed at 800 nm (1.55 eV) and a timescale from 125 fs to 1.5 ps showed that for this laser energy the yield becomes negligible small as the pulse duration tends toward 1.5 ps. The yield data were fitted by a power law Y~F^p, with p ranging from 7.3 to 9.1, yield raising with the pulse duration. These exponents are close to the value 8 ± 1 obtained in the CO/Cu(100) desorption or the value 7.2 ± 0.5 obtained in the closely related experiment performed on CO/O_2/Pt(111) [105]. These similarities between CO/Pt and CO/Cu systems together with the nearly identical vibrational lifetimes points out to a very similar energy transfer in the two systems. However, theoretical calculations for the CO/Pt desorption are so far missing.

First-principles electronic structure calculations [106] with configuration interaction (HONDO program) performed on small CO/Pt(111) and NO/Pt(111) clusters showed the existence of unoccupied anti-bonding orbitals of σ symmetry, with energies close to those of $2\pi^*$-derived orbitals (bonding and anti-bonding), considered to correspond to what has been identified as the $5\sigma_a$-derived band in an inverse photoemission study. Also, the electronic adiabatic model of Jennison [107,108] showed that the $2\pi^*$ state is heavily mixed with several lower repulsive states in the equilibrium region. More recently, based on temperature (CDM) calculations and application of the adiabatic model, Cai et al. [109] argued that the excitation of the anti-bonding state lead to desorption in the 800 nm experiment on CO/Pt. In this case, desorption follows the MGR-like instead of Antoniewicz-like scenario. Similarly, Saalfrank et al. [58] showed that is possible to account for the NO small vibrational excitation only assuming a partial negative charge on the NO in

the excited state. The nature of the excited state and the associated charge in CO and NO desorption from metal surfaces remain controversial until definitive experimental evidence will be presented.

5. Conclusions

With the advent of femtosecond laser pulses, a new generation of experiments involving formation of hot electrons at surfaces becomes possible. Desorption of adsorbates from metal surfaces can be achieved by such excitation of substrate electrons. The fluency dependence of desorption yield is highly nonlinear and the timescale for desorption has been established to be in the subpicosecond domain. These factors point out to a desorption mechanism that involves direct nonadiabatic couplings between the substrate electrons and nuclear degrees of freedom of adsorbate molecules.

In this review, we presented the theoretical work done to model the coupling between molecule degrees of freedom and the substrate hot electrons in connection with its efficiency in photodesorption. Two principal categories of models have been invoked to account for this femtosecond laser induced desorption. A first category, based on the generalization of DIET or DIMET models in the framework of the diabatic picture, favors the desorption mechanism based on the Antoniewicz-type scenario proposed by Gadzuk, and is build using a neutral ground state and a negative-ion resonance. Time-dependent density matrix theory, perturbation theory and wave packet methods offer a quantum mechanical framework describing the dynamics of a system coupled with a dissipative environment. An alternative approach is offered by the time-independent quantum theories. A second category is the adiabatic frame, consisting of the phenomenological description of the non-adiabatic coupling between the adsorbate nuclear motion and the hot electrons via an effective friction of electronic origin and a fluctuating force governed by an effective temperature of the hot electrons. The assumption implicit in the frictional model is the electron-electron thermalization occurring faster than either non-adiabatic coupling to lattice phonons or adsorbate degrees of freedom. This assumption was used, however, also in the diabatic picture where excitation or deexcitation rates dependent on the electronic temperature were considered. Whether such a thermodynamic equilibrium is really reached in desorption experiments is still an open question. Experiments [97,98,110-113] and a theoretical study [99] performed on gold surfaces showed that the electronic distribution function is far from equilibrium in the subpicosecond regime. Experimental tests on other surfaces would clarify the situation.

Although the existing models can explain a surprisingly high number of experimental observations, they are still crude and many refinements are necessary for a detailed microscopic understanding of the mechanism. Possible refinements include more precise potential energy surfaces especially for the excited state, a detailed inclusion of metal band structure, of lattice vibrations and of interactions between phonons and electrons. For the adsorbate, one should include hindered rotation or translation or coverage dependent quenching rates. The goal should be a theory that not only explains the yield dependence or the final-state distribution but also predicts them prior to the experiments. One of the most important output of the theory will be in molecular nano-devices [117], catalysis and gas sensors [125].

Acknowledgements

The author thanks Georges Raseev for his contribution and many helpful discussions.

References

[1] M. J. Feldstein, P. Vöringer, W. Wang, N. F. Scherer, J. Phys. Chem. **100**, 4739 (1996).
[2] J. A. Prybyla, H. W. Tom, G. D.Aumiller, Phys. Rev. Lett. **68**, 503 (1992).
[3] S. Funk, M. Bonn, D. N. Denzler, Ch. Hess, M. Wolf, G. Ertl, J. Chem. Phys. **112**, 9888 (2000).
[4] T. J. Chuang, Surf. Sci. Rep. **3**, 1 (1983).

[5] X. L. Zhou, X. Y. Zhu, J. M. White, Surf. Sci. Rep. **13**, 73 (1991).
[6] F. M. Zimmerman, W. Ho, Surf. Sci. Rep. **22**, 127 (1995).
[7] H. L. Dai, W. Ho, Laser Spectroscopy and Photochemistry on Metal Surfaces, World Scientific, Singapore (1995).
[8] H. Guo, P. Saalfrank, T. Seidemar, Prog. Surf. Sci. **62**, 239 (1999).
[9] J. A. Prybyla, T. F. Heinz, J. A. Misewich, M. M. T. Loy, G. H. Glownia, Phys. Rev. Lett. **64**, 1537 (1990).
[10] F. Budde, T.F. Heinz, M.M.T. Loy, J. A. Misewich, F. de Rougemont, H. Zacharias, Phys. Rev. Lett. **66**, 3024 (1991).
[11] F. Budde, T.F. Heinz, A. Kalamarides, M.M.T. Loy, J. A. Misewich, Surf. Sci. **283**, 143 (1993).
[12] S. A. Buntin, L. J. Richter, R. R. Cavanagh, D. S. King, Phys. Rev. Lett. **61**, 1321 (1988).
[13] S. A. Buntin, L. J. Richter, R. R. Cavanagh, D. S. King, J. Chem. Phys. **91**, 6429 (1989).
[14] J. W. Gadzuk, L. J. Richter, S. A. Buntin, D. S. King, R. R. Cavanagh, Surf. Sci. **235**, 317 (1990).
[15] L. M. Struck, L. J. Richter, S. A. Buntin, R. R. Cavanagh, J. C. Stephenson, Phys. Rev. Lett. **77**, 4576 (1996).
[16] A. Peremans, K. Fukutani, K. Mase, Y. Murata, Phys. Rev. B **47**, 4135 (1993).
[17] A. Peremans, K. Fukutani, K. Mase, Y. Murata, Surf. Sci. **283**, 189 (1993).
[18] L. Cai, X. Xiao, M. M. T. Loy, Surf. Sci. Lett. **464**, L727 (2000).
[19] J. A. Misewich, A. Kalamarides, T. F. Heinz, U. Höfer, M. M. T. Loy, J. Chem. Phys. **100**, 736 (1994).
[20] J. A. Misewich, S. Nakabayashi, P. Weigand, M. Wolf, T. F. Heinz, Surf. Sci. **363**, 204 (1996).
[21] F. Weik, A. de Meijere, E. Haselbrink, J. Chem. Phys. **99**, 682 (1993).
[22] F. J. Kao, D. G. Busch, D. Cohen, D. Gomes da Costa, W. Ho, Phys. Rev. Lett. **71**, 2094 (1993).
[23] D. G. Busch, S. Gao, R. A. Pelak, M. F. Booth, W. Ho, Phys. Rev. Lett. **75**, 673 (1995).
[24] T. Hertel, M. Wolf, G. Ertl, J. Chem. Phys. **102**, 3414 (1995).
[25] R. Haight, Surf. Sci. Rep. **21**, 275 (1995).
[26] D. Menzel, R. Gomer, J. Chem. Phys. **41**, 3311 (1964).
[27] P. A. Readhead, Can. J. Phys. **42**, 886 (1964).
[28] P. R. Antoniewicz, Phys. Rev. B **21**, 3811 (1980).
[29] Z. W. Gortel, R. Teshima, H. J. Kreuzer, Phys. Rev. B **37**, 3183 (1988).
[30] Z. W. Gortel, M. Tsukada, Phys. Rev. B **39**, 11259 (1989); Z. W.Gortel, Surf. Sci. **231**, 193 (1990).
[31] W. Hübner, W. Brenig, Z. Phys. B **74**, 361 (1989).
[32] Z. W. Gortel, A. Wierzbicki, Surf. Sci. Lett. **239**, L565 (1990); Phys. Rev. B **43**, 7487 (1991).
[33] Z. W. Gortel, R. Teshima, H. J. Kreuzer, Phys. Rev. B **47**, 9825 (1993).
[34] Ph. Avouris, R. Kawai, N. D. Lang, D. M. Newns, J. Chem. Phys. **89**, 2388 (1988).
[35] J. W. Gadzuk, Surf. Sci. **342**, 345 (1995).
[36] J. W. Gadzuk, C. W. Clark, J. Chem. Phys. **91**, 3174 (1989).
[37] J. W. Gadzuk, Ann. Rev. Phys. Chem. **39**, 395 (1988).
[38] P. Schuck, W. Brenig, Z. Phys. B **46**, 137 (1982).
[39] E. J. Heller, J. Chem. Phys. **62**, 1544 (1975); J. Chem. Phys. **64**, 63 (1976).
[40] J. A. Misewich, T. F. Heinz, D. M. Newns, Phys. Rev. Lett. **68**, 3737 (1992).
[41] H. Guo, J. Chem. Phys. **106**, 1967 (1997).
[42] H. Guo, Li Liu, Surf. Sci. **372**, 337 (1997).
[43] Li Liu, H. Guo, T. Seideman, J. Chem. Phys. **104**, 8757 (1996).
[44] P. Saalfrank, Chem. Phys. **193**, 119 (1995).
[45] H. Tal-Ezer, R. Kosloff, J. Chem. Phys. **81**, 3967 (1984).
[46] M. D. Feit, J. A. Fleck, A. Steger, J. Comput. Phys. **47**, 412 (1982); R. Kosloff, J. Phys. Chem. **92**, 2087 (1988).
[47] M. Monnerville, B. Duguay, J. C. Rayez, J. Chim. Phys. **87**, 843 (1990).
[48] J. Stromquist, S. Gao, J. Chem. Phys. **106**, 5751 (1997).

[49] D. Bejan, G. Raseev, M. Monnerville, Surf. Sci. **470**, 293 (2000).
[50] D. Bejan, G. Raseev submitted to J. Phys. C.
[51] S. M. Harris, S. Holloway, G. R. Darling, J. Chem. Phys. **102**, 8235 (1995).
[52] P. Saalfrank, R. Baer, R. Kosloff, Chem. Phys. Lett. **230**, 463 (1994).
[53] K. Blum, Density Matrix Theory and Applications, Plenum Press, New York (1981).
[54] P. Saalfrank, Chem. Phys. **211**, 265 (1996).
[55] P. Saalfrank, R. Kosloff, J. Chem. Phys. **105**, 2441 (1996).
[56] K. Finger, P. Saalfrank, Chem. Phys. Lett. **268**, 291 (1997).
[57] P. Saalfrank, Surf. Sci. **390**, 1 (1997).
[58] P. Saalfrank, G. Boendgen, K. Finger, L. Pesce, Chem. Phys. **251**, 51 (2000).
[59] G. Lindblad, Comm. Math. Phys. **48**, 119 (1976).
[60] J. M. Jean, R. A. Friesner, G. R. Fleming, J. Chem. Phys. **96**, 5827 (1992).
[62] B. Hellsing, H. Metiu, Chem. Phys. Lett. **127**, 45 (1992).
[63] I. Burghart, J. Phys. Chem. A **102**, 4192 (1998).
[64] M. Berman, R. Kosloff, H. Tal-Ezer, J. Phys. A **25**, 1283 (1992).
[65] W. Huisinga, L. Pesce, R. Kosloff, P. Saalfrank, J. Chem. Phys. **110**, 5538 (1999).
[66] H. Guo, R. Chen, J. Chem. Phys. **110**, 6626 (1999).
[67] S. I. Anisimov, B. L. Kapeliovici, T. L. Perel'man, Sov. Phys. JETP **39**, 375 (1974).
[68] D. A. Micha, Z. Yi, J. Chem. Soc. Faraday. Trans. **93**, 969 (1997).
[69] Z. Yi, D. Micha, J. Sund, J. Chem. Phys. **110**, 10562 (1999).
[70] S. Gao, B. I. Lundqvist, W. Ho, Surf. Sci. **341**, L1031 (1995).
[71] S. Gao, Phys. Rev. B **55**, 1876 (1997).
[72] T. Seideman, J. Chem. Phys. **106**, 417 (1997).
[73] T. Seideman, H. Guo, J. Chem. Phys. **107**, 8627 (1997).
[74] H. Haken, Light, vol. 1, North-Holland Physiscs Publishing, Amsterdam (1986).
[75] F. Dzegilenko, E. Herbst, J. Chem. Phys. **100**, 9205 (1994).
[76] F. Dzegilenko, E. Herbst, J. Chem. Phys. **104**, 6330 (1996).
[77] E. Hasselbrink, Chem. Phys. Lett. **170**, 329 (1990).
[78] C. Springer, M. Head-Gordon, J. C. Tully, Surf. Sci. **320**, L57 (1994).
[79] C. Springer and M.Head-Gordon, Chem. Phys. **205**, 73 (1996).
[80] M. Head-Gordon, J. C. Tully, J. Chem. Phys. **103**, 10137 (1995).
[81] M. Brandbyge, P. Hedegard, T. F. Heinz, J. A. Misewich, D. M. Newns, Phys. Rev. B **52**, 6042 (1995).
[82] X. Guo, J. Yoshinobu, J. Yates, Jr., J. Chem. Phys. **92**, 4320 (1990).
[83] J. Yoshinobu T. H. Ballinger, Z. Xu, H.J. Jänsch, M. I. Zaki, J. Xu, J. Yates, Surf. Sci. **255** (1991).
[84] A. Asscher, F. M. Zimmerman, L. L. Sprinsteen, P. L. Houston, J. Chem. Phys. **96**, 4808 (1992).
[85] K. Al-Shamery, I. Beauport, H. J. Freund, H. Zacharias, Chem. Phys. Lett. **222**, 107 (1994).
[86] P. Kronauer, D. Menzel, Adsorption-desorption phenomena, Academic Press, New York (1972).
[87] P. Feulner, D. Menzel, H. J. Kreuzer, Z. W. Gortel, Phys. Rev. Lett. **53**, 671 (1984).
[88] S. Wurm, P. Feulner, D. Menzel, Surf. Sci. **400**, 155 (1998).
[89] L. Bartels, G. Meyer, K. H. Rieder, D. Velic, E. Knoesel, A. Hotzel, M. Wolf, G. Ertl, Phys. Rev. Lett. **80**, 2004 (1998).
[90] G. A. Somorjai, Introduction to Surface Chemistry and Catalysis, John Wiley and Sons, New York (1994).
[91] J. C. Tully, M. Gomez, J. Vac. Sci. Technol. A **11**, 1914 (1993).
[92] J. T. Kindt, J. C. Tully, Surf. Sci. **477**, 149 (2001).
[93] B. E. Hayden, D.C. Godfrey, J. Elect. Spect. Rel. Phenom. **45**, 351 (1987).
[94] J. K. Brown, A. C. Luntz, Chem. Phys. Lett. **204**, 451 (1993).
[95] S. Gao, Surf. Sci. **313**, 448 (1994).
[96] K. Hasegawa, H. Kasai, W. A. Dino, A. Okiji, Surf. Sci. **438**, 283 (1999).
[97] W. S. Fann, R. Storz, H. W. K. Tom, J. Bokor, Phys. Rev. Lett. **68**, 2834 (1992).
[98] W. S. Fann, R. Storz, H. W. K. Tom, J. Bokor, Phys. Rev. B **46**, 13592 (1992).

[99] D. Bejan, G. Raseev, Phys. Rev. B **55**, 4250 (1997).
[100] M. Wolf, A. Hotzel, E. Knoesel, D. Velic, Phys. Rev. B **59**, 5926 (1999).
[101] G. Raseev, D. Bejan, Surf. Sci. **528**, 196 (2003).
[102] D. Bejan, G. Raseev, Surf. Sci. **528**, 163 (2003).
[103] T. Vondrak, X. Y. Zhu, Phys. Rev. Lett. **82**, 1967 (1999).
[104] S. Ogawa, H. Petek, Surf. Sci. **357-358**, 585 (1996).
[105] F. H. Her, R. J. Finlay, C. Wu, E. Mazur, J. Chem. Phys. **108**, 8595 (1998).
[106] H. Aizawa, S. Tsuneyuki, Surf. Sci. **363**, 223 (1996).
[107] D. R. Jennison, E. B. Stechel, A. R. Burns, Y. S. Li, Nucl. Instr. Meth. Phys. Res. B **101**, 22 (1995).
[108] D. R. Jennison, E. B. Stechel, A. R. Burns, in Laser Spectroscopy and Photochemistry on Metal Surfaces, World Scientific, Singapore (1995).
[109] L. Cai, X. Xiao, M. M. T. Loy, Surf. Sci. Lett. **492**, L688 (2001).
[110] R. W. Schoenlein, W. Z. Lin, J. G. Fujimoto, G. L. Easley, Phys. Rev. Lett . **58**, 1680 (1987).
[111] S. D. Brorson, W. Z. Lin, J. G. Fujimoto, E. P. Ippen, Phys. Rev. Lett. **59**, 1962 (1987).
[112] R. H. M. Groenveld, R. Sprik, Ad Lagendijk, Phys. Rev. B **45**, 5079 (1992).
[113] R. H. M. Groenveld, R. Sprik, Ad Lagendijk, Phys. Rev. B **51**, 11433 (1995).
[114] H. Guo, G. Ma, J. Chem. Phys. **111**, 8595 (1999).
[115] H. Guo, G. Ma, Surf. Sci. **451**, 7 (2000).
[116] P. T. Howe, H. L. Dai, Surf. Sci. **451**, 12 (2000).
[117] T. Seideman, J. Phys. C **15**, R521 (2003).
[118] M. Morin, N. J. Levinos, A. L. Harris, J. Chem. Phys. **96**, 3950 (1992).
[119] J. W. Gadzuk, Phys. Rev. B **44**, 13466 (1991).
[120] H. Guo, T. Seideman, J. Chem. Phys. **103**, 9062 (1995).
[121] H. Guo, Chem. Phys. Lett., **240**, 393 (1995).
[122] H. Guo, F. Chen, Faraday Disc. Chem. Soc. **108**, 309 (1997).
[123] P. Saalfrank, S. Holloway, G. R. Darling, J. Chem. Phys. **103**, 6720 (1995).
[124] M. Torri, Z. W. Gortel, R. Teshima, Phys. Rev. B **58**, 13982 (1999).
[125] S. Capone, A. Forelo, L. Francioso, R. Rella, P. Siciliano, J. Spadavecchia, D. S. Presicce, A. M. Taurino, J. Optoelectron. Adv. Mater. **5**(5), 1335 (2003).